Journal of Thermal Analysis and Calorimetry, Vol. 95 (2009) 2, 361–367

LIQUID–SOLID METASTABLE PHASE EQUILIBRIA FOR THE QUATERNARY SYSTEM ($NaCl–KCl–CaCl_2–H_2O$) AT 308.15 K

D. C. Li[1,2] *and T. L. Deng*[1,2*]

[1]College of Materials, Chemistry and Chemical Engineering, Chengdu University of Technology, Chengdu 610059, P.R. China
[2]Key Laboratory of Salt Lake Resources and Chemistry at Qinghai Institute of Salt Lakes, Chinese Academy of Sciences
Xining 810008, P.R. China

The solubility and the physicochemical properties (densities, viscosities, refractive indices, conductivities and pH) in the liquid–solid metastable system ($NaCl–KCl–CaCl_2–H_2O$) at 308.15 K have been investigated using the isothermal evaporation method, and the dry-salt phase diagram, water-phase diagram, and the diagram of physicochemical properties *vs.* composition in the system were plotted. One three-salt cosaturated point, three metastable solubility isotherm curves, and three crystallization regions corresponding to sodium chloride, potassium chloride and calcium chloride tetrahydrate were formed, and neither solid solution nor double salts were found. On the basis of the extended Harvie–Weare (HW) model and its temperature-dependent equation, the values of the Pitzer parameters $\beta^{(0)}$, $\beta^{(1)}$, C^{ϕ} for NaCl, KCl and $CaCl_2$, the mixing ion-interaction parameters $\theta_{Na,K}$, $\theta_{Na,Ca}$, $\theta_{K,Ca}$, $\Psi_{Na,K,Cl}$, $\Psi_{Na,Ca,Cl}$, $\Psi_{K,Ca,Cl}$, and the Debye–Hückel parameter A^{ϕ} and the chemical potentials of the minerals in the quaternary system at 308.15 K were fitted, and the predictive solubility based on the temperature-dependent equation and the chemical potentials of the minerals agrees well with the experimental data.

Keywords: *metastable phase equilibrium, Pitzer parameters, solubility*

Introduction

There are more than seven hundred salt lakes, each with an area larger than 1 km^2, in the Qinghai–Tibet Plateau, China, and brines with high concentrations of potassium and boron are widely distributed in the Qaidam Basin of the Qinghai–Tibet Plateau. Recently, a huge unique store of oil-field brine was also discovered in the Nanyishan Section in the Qaidam Basin. The hydrochemistry of the oilfield brine is of the calcium chloride type with a high concentration of sodium, potassium, lithium, borate and calcium [1]. The brine mostly belongs to the complex six-component system of ($Li–Na–K–Ca–Cl–B_4O_7–H_2O$).

It is well known that the phase equilibria of brine-mineral play an important role in exploiting brine resources and in describing geochemical evolution of brine ore. Although all these oilfield brine resources are very valuable, nothing has been reported on potential multipurpose utilization because of a lack data on the relative solubilities and phase diagram of the cadmium-bearing systems, especially thermodynamic data on metastable equilibria. In order to exploit these stores of oilfield brine, it is essential to make use of local climatic resources such as wind and solar pond techniques. The climate in the region of the Qaidam Basin is windy, aridly, little rainfall, so providing great evaporating capacity [2]. Therefore, the metastable phase equilibrium studied in the laboratory in conditions similar to those occurring naturally can objectively describe the interaction between brine and minerals and reveal the crystallization path of the various salts.

The quaternary system ($NaCl–KCl–CaCl_2–H_2O$) is a subsystem of the six-component system. Although the metastable phase equilibria of the subsystem ($KCl–CaCl_2–H_2O$) at (288.15 and 308.15) K [3] and some stable phase equilibria of the ternary subsystems on the quaternary system between 273.15 and 373.15 K have previously been reported [4–8], there are no reports in the literature concerning either stable or metastable equilibria of the quaternary system at 308.15 K. In this paper, the metastable solubility and physicochemical property data of the quaternary system at 308.15 K were determined with the isothermal evaporation method, and the predictive solubilities based on the Pitzer ion interaction model and its extended Harvie–Weare (HW) model have been successfully predicted.

Experimental

Apparatus and reagents

The isothermal evaporation equipment was designed in our laboratory. In an air-conditioned laboratory, a

---

[*] Author for correspondence: tldeng@isl.ac.cn

1388–6150/$20.00

Akadémiai Kiadó, Budapest, Hungary
Springer, Dordrecht, The Netherlands

thermally insulated box (70 cm long, 65 cm wide, 60 cm high) was fitted with an electric fan to control the temperature. The control system consisted of three parts: an electric relay, an electrical contact thermograph and heating lamps. When the solution temperature in the vessel was below 308.15 K, the apparatus for controlling the temperature formed a circuit and the heating lamps began to heat. Conversely, the circuit was broken and the heating lamps stopped working when the temperature rose above 308.15 K. By this means, the solution temperature in the container could always be kept at 308.15±0.2 K. The electric fan installed in the box can accelerate the rate of evaporation of the solutions. The crystals of the solid phase were analyzed with a XP-300 Digital Polarizing Microscopy (Shanghai Caikon Optical Instrument Co. Ltd., China) and with an X-ray diffractometer (X'pert PRO, Spectris. Pte. Ltd., The Netherlands). A thermostat, which can automatically control the temperature, ensured that all physicochemical parameters were strictly measured at 308.15±0.1 K.

The chemicals used were of analytical purity grade and seriously re-crystallized before use. They are all obtained from the Tianjin Kermel Chemical Reagent Ltd.: sodium chloride (NaCl, 99.5 mass%), potassium chloride (KCl, 99.5 mass%) and calcium chloride ($CaCl_2 \cdot 2H_2O$, 98 mass%). Deionized distilled water (DDW) with conductivity less than $1.0 \cdot 10^{-4}$ S m^{-1} and pH 6.60 at room temperature was used to prepare the series of artificial brines and for chemical analysis.

Experimental methods

The isothermal evaporation method was used in this study. Depending on the phase equilibrium composition, the appropriate quantity of salts and DDW were calculated and mixed into clean polyethylene containers (15 cm in diameter, 6 cm high). After the salts had completely dissolved, the containers were put into the box for isothermal evaporation at 308.15±0.2 K. The evaporation conditions were controlled with air flowing at a velocity of 3.5–4.0 m s^{-1}, relative humidity of 20–30%, and an evaporation rate of 4–6 mm d^{-1}, Justas found in the climate of the Qaidam Basin. For metastable evaporation reasons, no stirring was applied to the solutions. The crystal behavior of solid phase was observed periodically. When enough new solid phase appeared, the wet residue mixtures were separated from the solution. Then one part of the solid phases was quantitatively dissolved using DDW and analyzed by chemical methods. The other part was slightly dried at 308.15±0.2, then observed using an XP-300D Digital Polarizing Microscopy, and further identified using an X-ray diffraction. The compositions of the liquid phase were analyzed by the chemical analysis methods. Take a 5.0 mL sample of the clarified solution from the liquid phase with a pipette, which was treated with filter and diluted to 250.0 mL final volume in a volumetric flask filled with DDW to determine the concentration of the liquid-phase components. Some other solutions which were taken from the containers with the same filter way were used to measure the corresponding physicochemical properties of solutions in this sampling. The remainder of the solution continued to be evaporated and reached a new metastable equilibrium.

Analytical methods

The concentration of K^+ was measured by gravimetric methods using sodium tetraphenyl borate. The average relative deviation of the determination was less than ±0.05%. The Ca^{2+} ion concentration was determined by titration with EDTA standard solution in the presence of alkali and Ca-indicator. The uncertainty was less than ±0.3%. The Cl^- ion concentration was measured by titration with hydrargyrum nitrate standard solution in the presence of mixed indicator of diphenylcarbazone and bromphenol blue (uncertainty ±0.3%), and Na^+ was analyzed by graphite furnace atomic absorption spectrometry (precision ±0.5 mass%, Medal HITACHI 180-80) and evaluated with the calculated result using ion balance [9].

The liquid-phase physicochemical properties density, viscosity, conductivity, refractive index and pH were measured. The pH value was measured with a PHS-3C precision pH meter supplied by the Shanghai Precision & Scientific Instrument Co., Ltd with a precision of ±0.01. The pH meter was calibrated with standard buffer solutions either mixing phosphate of potassium dihydrogen phosphate with sodium dihydrogen phosphate (pH 6.84) or borax (pH 9.18), respectively. The densities (ρ) were measured with a density bottle method with a precision of ±0.0002 g cm^{-3}. The viscosities (η) were determined using an Ubbelohde capillary viscometer, which was placed in a thermostat that electronically controlled the set temperature to 308.15±0.1 K. At least five flow times for each equilibrium liquid-phase solution were measured. A stopwatch with a precision of 0.1 s was used to determine the flowing time, and the results were averaged. An Abbe refractometer (model WZS-1) was used to measure the refractive index (n_D) with an accuracy of ±0.0001. The conductivities (κ) were measured on a conductivity meter (Orion 145A+) with an accuracy of ±0.001 S m^{-1}. All the measurements were maintained at 308.15±0.1 K through control of the thermostat.

Results and discussion

The metastable equilibrium experimental results of solubilities and the relevant physicochemical properties of the quaternary system (NaCl–KCl–$CaCl_2$–H_2O) at 308.15 K are presented in Tables 1 and 2, respectively. The ion concentration values in the metastable equilibrium solution are expressed in mass%. According to the experimental data in Table 1, the experimental metastable phase diagram of the system at 308.15 K is shown in Fig. 1.

The metastable phase diagram of the quaternary system in Fig. 1 consists of three crystallization fields, one invariant point (point E), three univariant curves, and three crystallized regions of single salts. Point E is the invariant point of three salts co-saturated. The three curves of the univariant solubility isotherms are corresponding to E_1E, E_2E and E_3E. The three crystallization regions are corresponding to sodium chloride (NaCl), potassium chloride (KCl), and calcium chloride tetrahydrate ($CaCl_2 \cdot 4H_2O$). The crystallized area of sodium chloride is the largest whereas that of calcium chloride tetrahydrate is the smallest because of its high solubility. These results indicate that sodium chloride is more easily to saturate and crystallize from solution in this system because of the strong salting-out effect of the calcium chloride tetrahydrate. Neither solid solutions nor double salts were found in the quaternary metastable system.

The water phase diagram of the system at 308.15 K was shown in Fig. 2. This diagram repre-

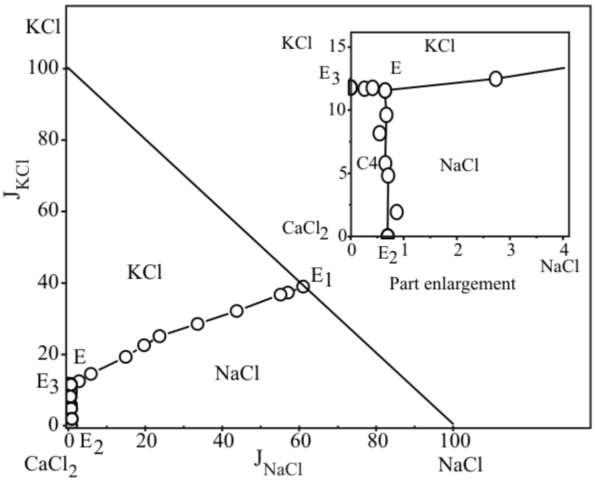

Fig. 1 Metastable phase diagram of the quaternary system (NaCl–KCl–$CaCl_2$–H_2O) at 308.15 K

Table 1 Solubility data of the metastable quaternary system (NaCl – KCl – $CaCl_2$ – H_2O) at 308.15 K

No.	Composition of liquid phase w/mass%			Composition of liquid phase Jänecke index, J_b(g/100 g S)			Equilibrium solid phase
	NaCl	KCl	$CaCl_2$	NaCl	$CaCl_2$	H_2O	
1,E_1	19.75	12.64	0.00	60.98	0.00	208.74	NaCl+KCl
2	18.40	12.04	1.83	57.02	5.67	209.89	NaCl+KCl
3	17.71	11.82	2.60	55.12	8.09	211.24	NaCl+KCl
4	14.40	10.59	7.93	43.74	24.09	203.77	NaCl+KCl
5	11.04	9.38	12.47	33.57	37.91	204.04	NaCl+KCl
6	7.82	8.29	16.90	23.69	51.20	202.94	NaCl+KCl
7	6.59	7.54	19.33	19.70	57.77	198.86	NaCl+KCl
8	5.14	6.64	22.69	14.91	65.83	190.11	NaCl+KCl
9	2.18	5.41	29.55	5.87	79.56	169.25	NaCl+KCl
10	1.20	5.48	37.21	2.73	84.78	127.84	NaCl+KCl
11,E	0.38	6.80	51.60	0.65	87.78	70.13	NaCl+KCl+C4*
12,E_2	0.32	0.00	51.08	0.69	99.30	93.39	NaCl+C4
13	0.45	1.01	50.50	0.87	97.19	92.46	NaCl+C4
14	0.38	2.60	50.90	0.71	94.47	85.60	NaCl+C4
15	0.36	3.21	51.74	0.65	93.55	80.80	NaCl+C4
16	0.30	4.52	50.42	0.54	91.27	81.03	NaCl+C4
17	0.38	5.44	50.68	0.67	89.70	76.99	NaCl+C4
18,E_3	0.00	6.79	50.72	0.00	88.19	73.90	KCl+C4
19	0.15	6.79	51.07	0.26	88.04	72.38	KCl+C4
20	0.24	6.87	51.23	0.41	87.81	71.41	KCl+C4

*C4, $CaCl_2 \cdot 4H_2O$

Table 2 Physicochemical property data of the quaternary system (NaCl – KCl – $CaCl_2$ – H_2O) at 308.15 K

No.*	pH	n_D	Conductivity κ/S m^{-1}	Viscosity 10^{-3} η/Pa s	Density ρ/g cm^{-3}
1,E_1	–	1.3869	–	–	1.2361
2	7.09	1.3896	–	1.1230	1.2388
3	7.06	1.3903	–	1.1643	1.2395
4	6.42	1.3960	–	1.2775	1.2544
5	6.62	1.4009	–	1.3951	1.2638
6	6.29	1.4060	–	1.5303	1.2829
7	6.10	1.4086	–	1.6600	1.2860
8	5.83	1.4136	–	1.7907	1.2984
9	5.43	1.4252	1.867	2.4604	1.3363
10	5.21	1.4454	1.338	5.1013	1.3960
11,E	4.75	1.4838	0.255	37.1093	1.6079
12,E_2	–	1.4678	–	–	1.5141
13	4.55	1.4661	0.618	–	1.4906
14	4.02	1.4658	0.568	–	1.4867
15	4.21	1.4745	0.377	18.8426	1.5304
16	4.40	1.4772	0.369	20.842	–
17	–	–	–	–	–
18,E_3	–	1.4815	–	–	1.5727
19	4.00	1.4756	0.366	20.9442	1.5765
20	4.45	1.4838	0.255	33.5113	1.5821

*The number order is in corresponding with Table 1

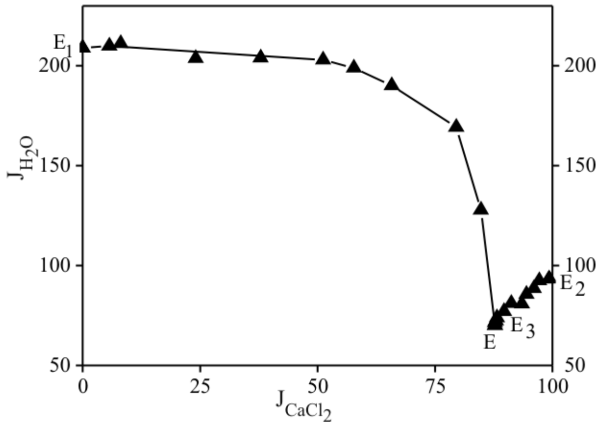

Fig. 2 Water phase diagram of the system (NaCl–KCl–$CaCl_2$–H_2O) at 308.15 K

sents the projection of the univariant curves (diagram of Jänecke) of the system (NaCl–KCl–$CaCl_2$–H_2O) at 308.15 K. It shows that the Jänecke index of water gradually decrease with increasing $CaCl_2$ index. On the basis of the experimental data in Table 2, the relationship diagrams of the solution physicochemical properties *vs.* the composition of solution in mass fractions were shown in Fig. 3. It can be seen that the physicochemical properties of the equilibrium solution change regularly with the mass fraction change of calcium chloride in the system. The densities, viscosities and refractive indexes of the aqueous solutions gradually increase with increasing calcium chloride concentration, reaching the maximum value at cosaturation point E in Fig. 3a–c. Whereas the trend for the conductivities of the aqueous solutions is reversed and the cosaturation point E has the minimum value in Fig. 3e. The pH values of the metastable equilibrium aqueous solution were in decreasing gradually with the increasing of calcium chloride concentration on the whole, and reach the singularity point at the co-saturation point E with pH value 4.75 in Fig. 3d.

Solubility prediction

Ion-interaction model

Pitzer *et al.* [10, 11] have developed an ion interaction model and published a series of papers, which gave a set of expressions for the osmotic coefficients of the solution and mean activity coefficient of electrolytes in the solution. Expressions of the chemical equilibrium model for conventional single ion activity coefficients derived by Harvie [12, 13] are more conve-

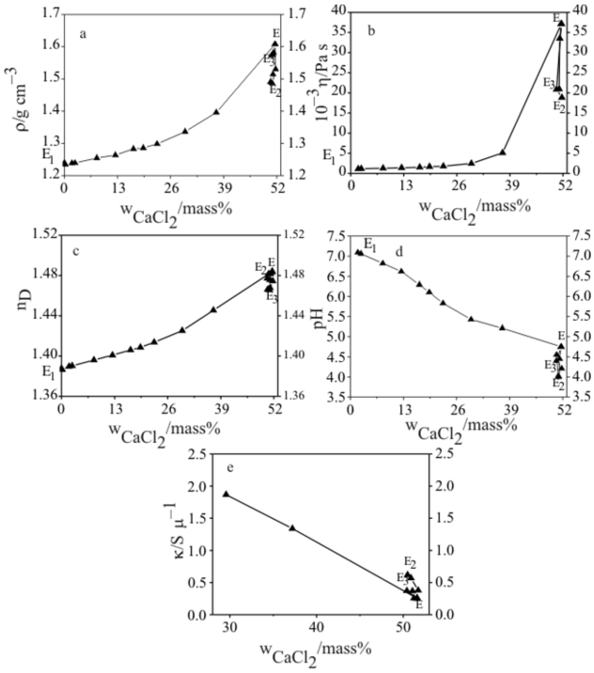

Fig. 3 Physicochemical properties with composition in the metastable quaternary system ($NaCl–KCl–CaCl_2–H_2O$) at 308.15 K. ▲ – experimental value; – – experimental relationship diagram; a – density; b – viscosity; c – refractive index; d – pH and e – conductivity *vs.* composition

nient to use in solubility calculations. Using the activity coefficients and the solubility products of the equilibrium solids phase allowed us to identify the coexisting solid phases and their compositions at equilibrium. Addition work has centered on developing variable temperature models, which will increase the applicability to a number of diverse geochemical systems. The primary focus has been to broaden the models in order to generate parameters at higher or lower temperatures [14–18].

Model parametrization

A high temperature thermochemical model for the system $Na–K–Ca–Cl–SO_4–H_2O$ is presented by Greenberg and Møller [16], which concentrated electrolyte solutions over temperature ranges from 273.15 to 523.15 K. Chemical potentials for the reactions of mineral solids and solutions were fitted simultaneously with the solution model parameters. The temperature-dependent equation and the free energy equation of the salt minerals for the system are shown as follows:

$$P(T)=a_{1+}a_2T+a_3/T+a_4\ln T+a_5/(T-263)+a_6T^2+a_7/(680-T)+a_8/(T-227)$$

$$\frac{\partial G}{\partial n_i}=\mu_i=\mu_i^0+RT\ln\gamma_i m_i$$

where in the first equations, $P(T)$ refers to the parameters of the solution model: the limiting law term of Debye–Hückel parameter A^ϕ, the Pitzer single salt parameters $\beta^{(0)}$, $\beta^{(1)}$, C^ϕ, and the mixed salt parameters θ, Ψ; the values of the fitting constant terms of a_1, a_2, a_3, a_4, a_6 and a_9 were introduced by Spencer [17]. While in the second equation, n_i and μ_i^0 are the number of moles of species *i* and the standard chemical potentials of species *i* in solution, γ_i and m_i are the activity coefficient and molality of solute species *i* in an electrolyte solution. Based on above equations, Pitzer single-salt parameters $\beta^{(0)}$, $\beta^{(1)}$, C^ϕ for NaCl, KCl and $CaCl_2$, Pitzer mixing ion-interaction parameters $\theta_{Na,K}$, $\theta_{Na,Ca}$, $\theta_{K,Ca}$, $\Psi_{Na,K,Cl}$, $\Psi_{Na,Ca,Cl}$, $\Psi_{K,Ca,Cl}$, Debye–Hückel parameter A^ϕ and the standard chemical potentials μ_r^0/RT for the minerals of NaCl, KCl, $CaCl_2·4H_2O$ and H_2O in the system at 308.15 K were fitted in Tables 3 and 4, respectively. By the way, more discussion on the chemical potentials of three different hydrates of calcium chloride ($CaCl_2·nH_2O$, n=6, 4, 2) was introduced in Christov and Møller [19].

Table 3 Single salt and mixing ion-interaction parameters in the solution of the quaternary system at 308.15 K

Single salts	$\beta^{(0)}$	$\beta^{(1)}$	C^ϕ
NaCl	8.191E-2	2.854E-1	4.047E-4
KCl	5.330E-2	2.316E-1	–1.131E-3
$CaCl_2$	3.067E-1	1.747E0	6.604E-4

A^ϕ	$\theta_{Na,K}$	$\theta_{Na,Ca}$	$\theta_{K,Ca}$	$\Psi_{Na,K,Cl}$	$\Psi_{Na,Ca,Cl}$	$\Psi_{K,Ca,Cl}$
3.985E-1	–4.730E-3	5.000E-2	1.756E-1	–3.136E-3	–3.000E-3	–4.024E-2

Table 4 Data of the standard chemical potential of minerals of the quaternary system at 308.15 K

Species	NaCl	KCl	$CaCl_2·4H_2O$	H_2O
μ^0/RT	3.683E0	2.324E0	–1.116E2	–3.151E1

Table 5 Comparison of the experimental and calculated values in the invariant points of the quaternary system ($NaCl–KCl–CaCl_2–H_2O$) at 308.15 K

No.	Composition of liquid phase, w_b/mass %			Equilibrium solid phase
	NaCl	KCl	$CaCl_2$	
Experimental	0.38	6.80	51.60	$NaCl+KCl+CaCl_2·4H_2O$
Calculated using (μ^0/RT)	0.024	6.03	49.36	$NaCl+KCl+CaCl_2·4H_2O$

Calculated solubility

Based on Pitzer ion-interaction model and its extended HW models of aqueous electrolyte solution, the solubilities of the quaternary system at 308.15 K have been calculated by using the temperature-dependent equation and the chemical potentials of the minerals. In the basis of calculated solubilities, the comparisons of the metastable experimental phase diagram of the quaternary system at 308.15 K with the predictive phase diagrams were plotted in Fig. 4 with the dashed lines. Comparison between the calculated solubilities and the experimental results in the invariant point E were shown in Table 5.

The comparison between experimental data and calculated results in Fig. 4 also indicates that the calculated results are consistent with the experimental data. However there exists deviation between calculated and experimental data in the saturated area of sodium chloride and calcium chloride, the deviation might be due to some other kind of interaction between the sodium ion and calcium ion. Those results indicate that the parameters obtained from the temperature-dependent equation in this work are reliable and that the chemical potentials of the minerals evaluated using the extended HW models is capable of predicting the metastable equilibria in the quaternary system.

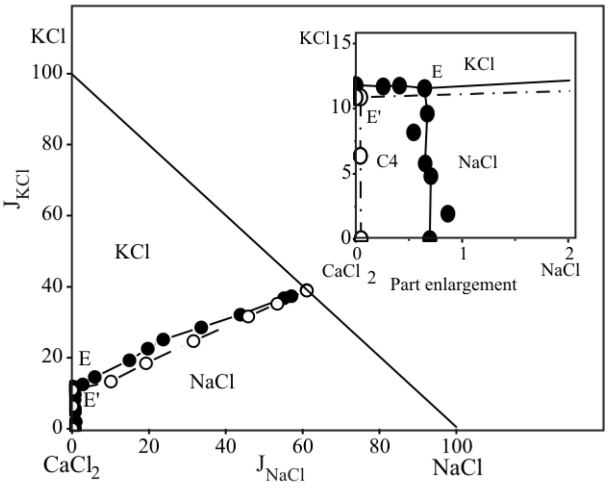

Fig. 4 Comparison of experimental and calculated (μ^0/RT) in metastable equilibrium phase diagram of the quaternary system at 308.15 K. ● – experimental value; ○ – calculated value; C4, $CaCl_2·4H_2O$

Conclusions

The solubilities and the physicochemical properties of the liquid-solid metastable quaternary system ($NaCl–KCl–CaCl_2–H_2O$) at 308.15 K were determined experimentally. According to the data, the experimental metastable phase diagram and the variation of the physicochemical properties with composition were constructed for the first time. Based on the temperature-dependent equation in the literature, Pitzer single-salt parameters, mixing ion-interaction parameters, the chemical potentials of the minerals in the system and Debye–Hückel parameter A^{ϕ} can be fitted smoothly. Solubility predictions for the quaternary system at 308.15 K have been made using the temperature-dependent equation and the chemical potentials of the minerals, the results demonstrate that Pitzer parameterizations based on the temperature-dependent equation and the chemical potentials of the minerals evaluated with the extended HW models are reliable in the quaternary system. The predictive metastable solubility with the extended HW models using the temperature-dependent equation and the standard chemical potentials of the minerals agrees well with the experimental data.

Acknowledgements

Financial supports from the State Key Program of National Natural Science of China (Grant. 20836009), the National Natural Science Foundation of China (Grants 40573044 and 40773045), the ‘A Hundred Talents Program’ of the Chinese Academy of Sciences (Grant 0560051057), and the Specialized Research Fund for the Doctoral Program of Chinese Higher Education (Grant. 20060616004) are greatly acknowledged. Authors also thank Professor Z. H. Gao, Associate Professor B. Sun, and Ms. P. Wang of Qinghai Institute of Salt-Lake for their valuable help. Thanks also to the Editor and the anonymous reviewers for their active comments on the manuscript.

References

1 J. L. Fu, S. S. Yu, S. J. Li and H. Y. Ren, J. Salt Lake Res., 13 (2005) 17.
2 X. Y. Zheng, Y. Tang and C. Xu, Tibet Saline Lake. Chin. Sci. Press, Beijing (1988).
3 T. L. Deng, D. C. Li and S. Q. Wang, J. Chem. Eng. Data, 53 (2008) 1007.
4 V. P. Il'inskii, N. A. Varypaev, K. E. Gitterman and N. E. Shmidt, Tr. Solyanoi Lab., Akad. Nauk SSSR, 7 (1936) 32.
5 E. I. Luk'yanova and D. N. Shoikhet, Tr. Gos. Inst. Prikl. Khim., 34 (1940) 16.
6 O. K. Yanat'eva, Zh. Obshch. Khim., 17 (1947) 1040.
7 G. O. Assarsson, J. Am. Chem. Soc., 72 (1950) 1437 and 1440.
8 T. Mayer, C. Prutton and C. W. Lightfoot, J. Am. Chem. Soc., 71 (1949) 1237.
9 Analytical laboratory of Qinghai Institute of Salt Lakes at CAS, The Analyses of Brines and Salts, 2nd Ed. Chin. Sci. Press, Beijing 1988.
10 K. S. Pitzer, J. Phys. Chem., 77 (1973) 268.
11 K. S. Pitzer, Semi-empirical equations for pure and mixed electrolytes. Thermodynamics, 3rd Ed. McGraw–Hill, New York 1995.
12 C. E. Harvie and J. H. Weare, Geochim. Cosmochim. Acta, 44 (1980) 981.
13 C. E. Harvie, N. Moller and J. H. Weare, Geochim. Cosmochim. Acta, 48 (1984) 723.
14 R. T. Pabalan and K. S. Pitzer, Geochim. Cosmochim. Acta, 51 (1987) 2429.
15 N. Moller, Geochim. Cosmochim. Acta, 52 (1988) 821.
16 J. P. Greenberg and N. Møller, Geochim. Cosmochim. Acta, 53 (1989) 2503.
17 R. J. Spencer, N. Moller and J. Weare, Geochim. Cosmochim. Acta, 54 (1990) 575.
18 A. R. Nazmi, T. Reinisch and H. J. Hinz, J. Therm. Anal. Cal., 91 (2008) 141.
19 C. Christov and N. Møller, Geochim. Cosmochim. Acta, 68 (2004) 3717.

DOI: 10.1007/s10973-008-9236-3